

Viscosities of slags—an overview

S. SEETHARAMAN*, K. MUKAI†, and DU SICHEN*

**Department of Materials Science and Engineering, Royal Institute of Technology, Stockholm, Sweden*

†*Department of Materials Science and Engineering, Kyushu Institute of Technology, Kitakyushu, Japan*

Viscosities of slags constitute an important physical property needed for an understanding of the mass transfer phenomena in metallurgical processes. Viscosity is also the key that leads to a better understanding of the structure of slags. It is wellknown that the viscosities of silicate slags decrease with the addition of basic oxides due to the breaking of the silicate network.

The measurements of slag viscosities often pose experimental challenges, especially to the choice of materials. The keynote lecture takes up the experimental problems and the various techniques adopted. Dynamic viscosity measurement, as a powerful tool towards an understanding of the kinetics of some high temperature reactions, is brought out.

A number of semi-empirical models have been developed to estimate the slag viscosities in the case of multicomponent slags. A critical survey of these models is presented in the lecture. Earlier models by Riboud *et al.*, Urbain *et al.* and Mills *et al.* have been developed further into a new generation of models. Some of the current important models are (1) Model by Iida *et al.* (2) CSIRO model (3) Pyroresearch Model (4) Model by Tanaka *et al.* (5) Model approach by Reddy *et al.* and (6) KTH-model. The predictions and capabilities of the various models are compared. Estimations of viscosities from thermodynamic data and prediction of liquidus temperatures from viscosities are presented.

The concept of surface viscosities with reference to slags and viscosities of two-phase mixtures are also taken up in the presentation.

Introduction

A knowledge of viscosities is of immense importance in the modelling of high temperature processes. Viscosities of slags constitute an important physical property needed for an understanding of the mass transfer phenomena in metallurgical processes. In CFD calculations of steelmaking and refining processes, it is imperative that reliable viscosity values of the slag and metal phases are fed in to the models in order to achieve a sensible convergence¹. In this context, lots of attention has been given to the measurements and modelling of slag viscosities in recent years²⁻⁸. Despite these efforts, it is to be admitted that it needs a more concerted effort in order to get a full understanding of the viscosities of slags and to have models that can provide reliable extrapolations of available viscosity data as functions of temperature and composition in the case of multicomponent slags. The present paper is intended to provide a bird's-eye view of the viscosities of slags and the impact of this property on slag modelling.

Viscosity is a very interesting property, even from a fundamental view point. Viscosity reflects the extent to which relative motion of adjacent liquid layers is retarded, and it can be generally regarded as a measure of internal friction of the liquid. As the slags are ionic in nature and as the extent of polymerization varies with the metal oxide contents in the slag, it can be surmized that the viscosities of slags are extremely sensitive to the size of the ions as well as to the electrostatic interactions, and thereby to the structure of slags. Viscosity in the case of pure silica with three-dimensional silica network is extremely high. With successive addition of basic oxides, the silicate network

breaks down and, consequently, the viscosity decreases gradually⁹. An inquiry into the viscosities of slags would throw much light on the structure of slags.

The present paper provides an overview of the structural dependence of viscosities, experimental methods for viscosity measurements, viscosity estimation models available today, and a comparison of their performances in predicting the slag viscosities. Due to the fact that this is an extensive field, the present paper limits itself to iron- and steelmaking slags and thus leaves out slags involved in non-ferrous metallurgy. The paper also gives a brief idea of the viscosities of two-phase mixtures. The concept of surface viscosities is taken up in the light of interfacial phenomena and discussed briefly.

Viscosity and thermodynamic properties

As mentioned earlier, viscous flow is related to the structure of the liquid. In discussing the mechanism for viscous flow, it can be expected that the viscosity is dependent upon the nearest-neighbour interactions and coordination numbers. Interionic forces in melts are characterized by the thermodynamic state of the system. Thus, viscosities of liquids can be considered to be linked to order-disorder phenomena, thereby being related to the structure of the liquid. In the case of silicate melts, the ordering phenomena, as characterized by enthalpies, point to the extent of polymerization, while the disorder is marked by the thermal entropy factor, which is likely to influence the directional flow. Born and Green¹⁰ suggest that the viscosities of liquids may be considered to consist of two parts: viz. the interatomic forces as well as thermal motion.

The present authors consider that even the thermal motion is indirectly an expression of the entropy of the system. Thus, viscosity can be considered in a conceptual way as an integral molar property of the system related to the structure and, thus, linked to the thermodynamic properties of the system.

The coupling of viscosities to thermodynamic properties has been pondered over by many authors¹¹⁻¹³. For example, McCauley and Apelian¹¹ proposed an equation based on the classic Clausius-Clapeyron equation to describe the viscosity-temperature relationships in Newtonian liquids. Iida *et al.*¹² correlated viscosities with the heats of mixing, while Morita *et al.*¹³ used the activity coefficients in their correlations. The computation of the viscosities of binary metallic systems from the corresponding unary data using the thermodynamics of mixing has been successfully worked out by two of the present authors¹⁴. Similar efforts in the case of binary silicate systems were made by Seetharaman *et al.*¹⁵. These authors considered the activation energies for viscous flow, ΔG^* for pure silicates similar to the thermodynamic Gibbs energies in analogy with Richardson's theory of ideal mixing¹⁶. This is illustrated in Figure 1.

In this figure, the pure silicates are presented on the two sides of the triangle, while the base represents the binary metal oxide system. The iso-silicate compositions are parallel to the base line. It would be logical to expect that, if the two silicates mix ideally along the iso-silicate line, the activation energy for viscous flow can be expected to vary linearly. Any deviation from this linearity may be the result of interactions between the ions depending on the ionic

sizes and charges. Based on this, a correlation was developed to evaluate the ΔG^* for viscous flow in the ternary system and the thermodynamics of mixing. This is shown in Equation [1]

$$\Delta G^* = U_{Z(MO \cdot SiO_2)} \Delta G^*_{Z(MO \cdot SiO_2)} + U_{Z(YO \cdot SiO_2)} \Delta G^*_{Z(YO \cdot SiO_2)} + 3X_{MO} \cdot X_{YO} (1 - X_{SiO_2}) \Delta^E G_{Mix} \quad [1]$$

Successful predictions of the viscosities of binary silicates could be worked out using this relationship. Sridhar *et al.*¹⁷ compared the results of such estimations with a few of the viscosity models available as well as the available experimental data. These authors found that the predictions compared well with experimental data in contrast to some of the models. One such comparison published by these authors is presented in Figure 2.

Viscosity-composition relationships

Pure SiO_2 consists of 3-dimensional interconnected networks of SiO_4^{4-} tetrahedra in which Si cations are joined together as rings or chains by bridging oxygens. As basic oxides are introduced, the network disintegrates gradually into smaller units, leading to the increase in the number of nonbridging oxygen and eventually free-oxygen ions, O^{2-} .

The viscosity of a silicate melt at a given temperature is dependent upon the structure of the liquid. Pure silica, with a 3-dimensional network of SiO_4 -tetrahedra has extremely high viscosity. As the basic oxides are added, the silicate network breaks down and the viscosity decreases rapidly. With the breakdown of the silicate network, viscosity of the melt gets lowered, as illustrated in Figure 3.

Most of the metallurgical slags contain relatively higher amounts of metal oxides and thus exhibit lower viscosities. Glasses, coal ash slags and magmas, on the other hand, have high silica contents and consequently a high degree of polymerization and high viscosities. Aluminates and phosphates have tetrahedral structures and link with silicate tetrahedra in the polymeric networks. But these would require extra positive charge (for example, Na^+ in the case of aluminate) or negative charge (for example, F^- in the case of phosphate) for balancing the electrical charges.

Ionic associations, cation and anion size effects

If the energetics of viscous flow are analogous to the thermodynamic properties, the changes in Gibbs energies due to strong interactions between various species in the system should be reflected in viscosity as well. Darken¹⁸ has shown that the second derivative of the excess Gibbs energy of mixing, with respect to composition in the case of a binary metallic system, termed 'excess stability', should reflect the tendencies for compound formation. Darken applied the excess stability concept to silicate systems like $CaO-SiO_2$ and $FeO-SiO_2$ and showed that the excess stability diagram for these systems showed peaks corresponding to the formation of stoichiometric compounds.

Aune *et al.*¹⁹ attempted a similar approach to the change of viscosities as a function of composition. The second derivative of the logarithm of viscosity composition would be a sensitive function that would reflect the associations in the liquid silicate melt. In the case of a number of binary silicate melts, the second derivative of the logarithm of viscosities with respect to composition showed peaks corresponding to the metasilicates indicating the existence

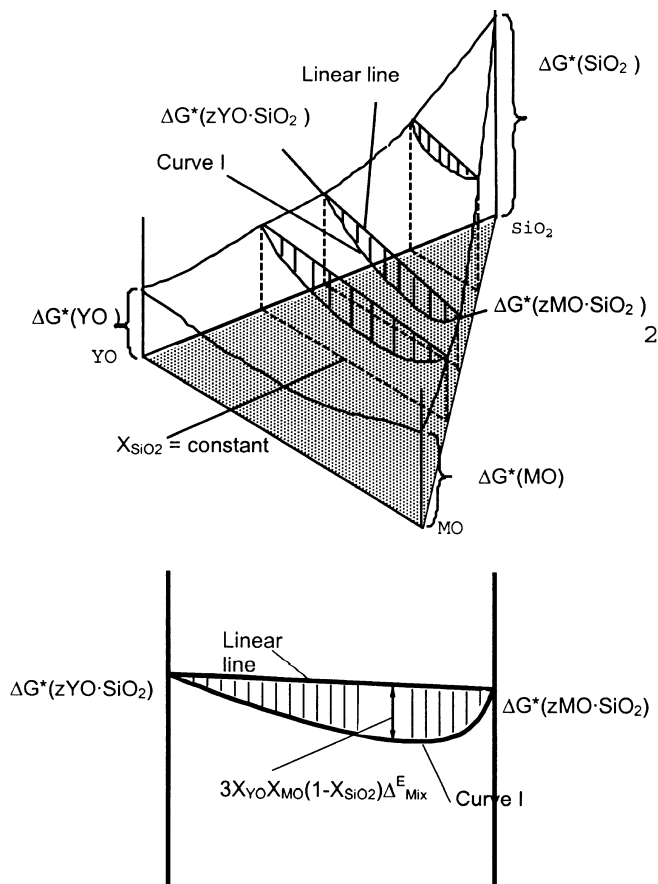


Figure 1. Gibbs activation energy surface for the viscosities of MO-YO- SiO_2 mixtures and a vertical section through the $zMO-SiO_2-zYO-SiO_2$

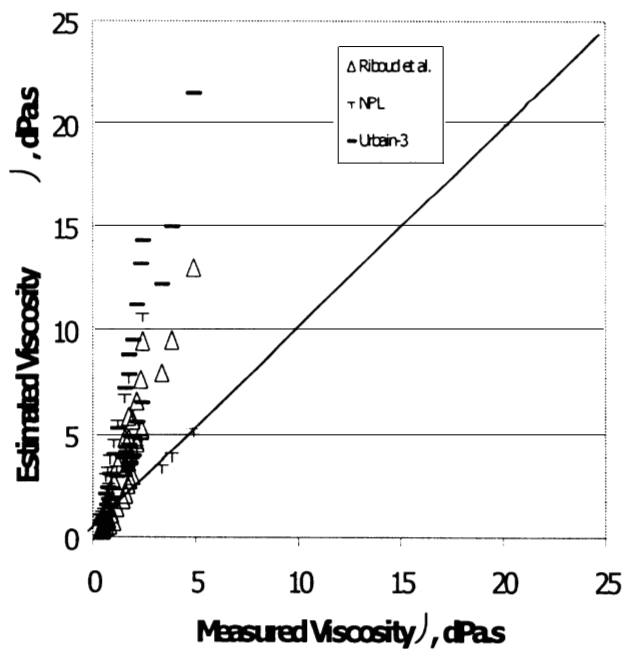
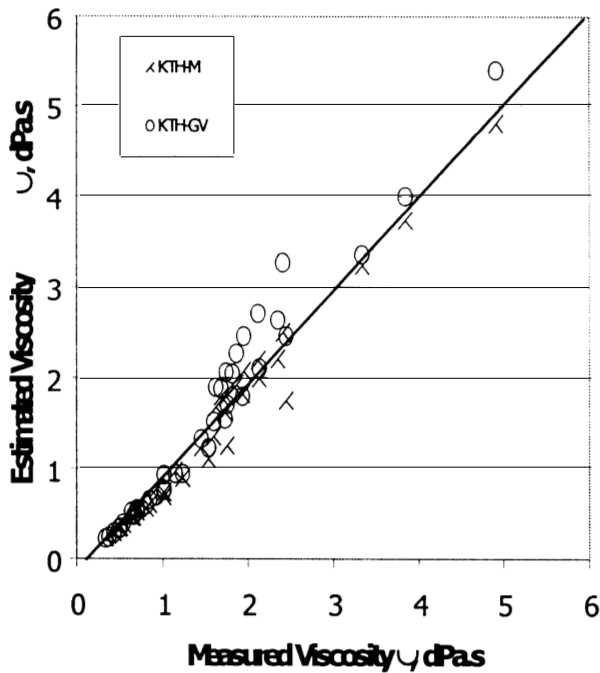


Figure 2. Estimated viscosities versus measured values for the system CaO-FeO-SiO₂

of associated species in the liquid state¹⁹. This is illustrated in the case of CaO-SiO₂ and MgO-SiO₂ melts in Figure 4.

Fujino and Morinaga²⁰ reported viscosity-temperature relations for 0.5MO-0.5P₂O₅ systems where M = Mg, Ca, Sr, Ba and Zn. According to these authors, viscosity values are in the hierarchy, MgO > ZnO > CaO > SrO > BaO i.e. inversely proportional to the radius of the cation. The activation energy increases with decreasing anion radius. This suggests that polymerization is greater in those melts containing small cations. Inspection of viscosity data for other systems, e.g. silicates, showed similar trends.

An inspection of the variation of viscosities at melting points for a variety of anionic complexes indicate that:

- viscosity values at the melting temperature (η^m) differ by almost 10³.

- viscosities are in the order, alumino-silicates > silicates > phosphates > boro-silicates = aluminates > borates > ferrites.

CaF₂ is widely used in industry to reduce the viscosity and the liquidus temperatures of the slag or glass. In the case of silicates, F⁻ causes the de-polymerization of the structure for slags with CaO/SiO₂ ratios of 1.0 and 1.3 by the formation of Si-F bonds. Extensive experimental work on the viscosities of silicate melts containing fluorides have been carried out in the Division of Metallurgy, Royal Institute of Technology, Stockholm. The viscosity changes due to addition of CaF₂ in the case of the systems CaO-SiO₂⁵, FeO-SiO₂⁶ as well as CaO-FeO-SiO₂⁷ were carried out by Fatemeh *et al.* These authors showed that the viscosities of CaO-FeO-SiO₂ slags are decreased drastically with the addition of CaF₂. This is illustrated in Figure 5.

It is very interesting to note that the extent of decrease in the viscosities caused by CaF₂ is a function of the slag basicities. It has been suggested in literature that, in the case of sodium and calcium silicates, fluorine enters into combination with SiO₂ at low basicities; but remains as F⁻ in basic melts⁹. The change role of CaF₂ as a function of basicity is illustrated in the case of the silicate melts FeO-SiO₂-CaF₂, wherein the FeO/SiO₂ ratio has a serious impact on the decrease of the activation energies for viscous flow due to CaF₂ additions. This is illustrated in Figure 6.

Temperature dependence of viscosities

The temperature dependence of the viscosity is usually expressed in one of the following forms of the Arrhenius relationship:

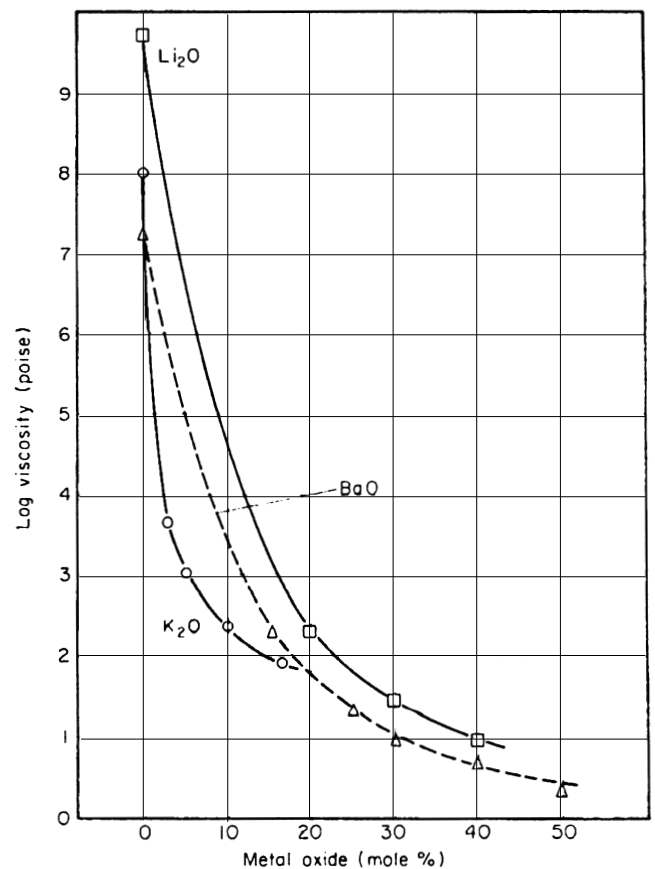


Figure 3. Viscosity of three binary silicate melts as a function of temperature⁹

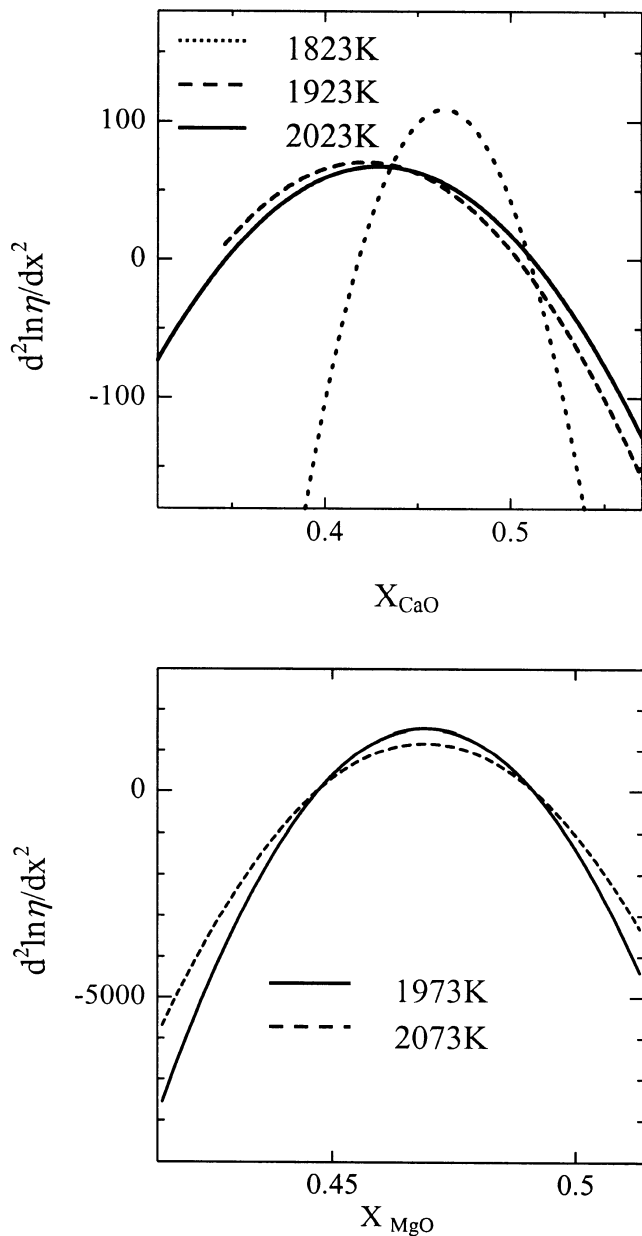


Figure 4. The second derivative of $\ln \eta$ with respect to composition in the case of CaO-SiO₂ and MgO-SiO₂ systems¹⁹

$$\eta = A_A \exp\left(\frac{E_A}{RT}\right) \quad [2]$$

where η is the viscosity, E the activation energy, R the gas constant, and T the temperature in K . Viscosity-temperature data are, on the basis of the above equations, usually presented in the form of $\ln \eta$ as a function of reciprocal temperature (T^{-1}).

It is, however, important to point out that the viscosity-temperature plots for silicates usually show a slight curvature. An improved fit can, in this case, be obtained by using the Wayman²¹ (3) and Brostow²² (4) relationships:

$$\eta = A_w T \exp\left(\frac{E_w}{RT}\right) \quad [3]$$

$$\eta = \exp\left(A_B + \frac{B_B}{T} + C_B \log T\right) \quad [4]$$

At lower temperatures, with the temperature approaching

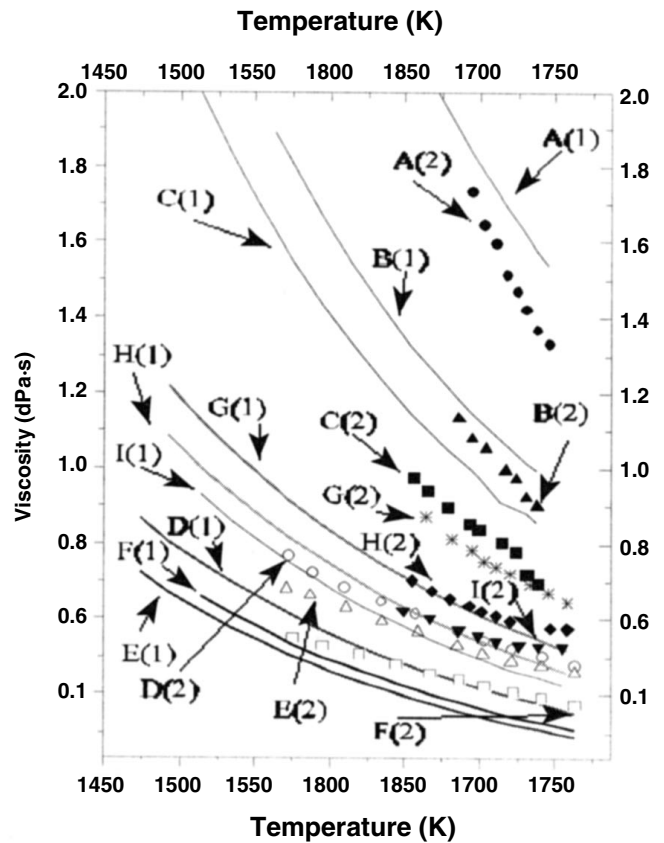


Figure 5. The variation of viscosity with temperature for some CaO-FeO-SiO₂-CaF₂ slags of different compositions. The solid lines represent corresponding silicate melts without CaF₂.

Slag No. 1-A(1): $X_{FeO}/X_{SiO_2}=1.045$, without CaF₂ A(2): $X_{FeO}/X_{SiO_2}=1.045$, $X_{CaF_2}=0.017$.
 Slag No. 2-B(1): $X_{FeO}/X_{SiO_2}=1.124$, without CaF₂. B(2): $X_{FeO}/X_{SiO_2}=1.124$, $X_{CaF_2}=0.0466$.
 Slag No. 3-C(1): $X_{FeO}/X_{SiO_2}=1.15$, without CaF₂. C(2): $X_{FeO}/X_{SiO_2}=1.15$, $X_{CaF_2}=0.057$.
 Slag No. 4-D(1): $X_{FeO}/X_{SiO_2}=1.94$, without CaF₂. D(2): $X_{FeO}/X_{SiO_2}=1.94$, $X_{CaF_2}=0.0157$.
 Slag No. 5-E(1): $X_{FeO}/X_{SiO_2}=2.17$, without CaF₂. E(2): $X_{FeO}/X_{SiO_2}=2.17$, $X_{CaF_2}=0.0465$.
 Slag No. 6-F(1): $X_{FeO}/X_{SiO_2}=2.02$, without CaF₂. F(2): $X_{FeO}/X_{SiO_2}=2.102$, $X_{CaF_2}=0.0739$.
 Slag No. 7-G(1): $X_{FeO}/X_{SiO_2}=1.54$, without CaF₂. G(2): $X_{FeO}/X_{SiO_2}=1.54$, $X_{CaF_2}=0.0156$.
 Slag No. 8-H(1): $X_{FeO}/X_{SiO_2}=1.575$, without CaF₂. H(2): $X_{FeO}/X_{SiO_2}=1.575$, $X_{CaF_2}=0.041$.
 Slag No. 9-I(1): $X_{FeO}/X_{SiO_2}=1.58$, without CaF₂. I(2): $X_{FeO}/X_{SiO_2}=1.58$, $X_{CaF_2}=0.0616$.

the freezing point, there is some ordering due to the rearrangements of ions in the melt as solidification is anticipated. This would result in departures from linearity in $\ln \eta - T^{-1}$ plots in contrast to the classical Arrhenius behaviour. Seetharaman *et al.*²³ have shown that the second differential with respect to temperature

$$\frac{\partial^2 Q}{\alpha T^2} \left(\frac{1}{R}\right) = \frac{\partial^2}{\partial T^2} \left[\frac{\partial(\ln \eta)}{\partial \left(\frac{1}{T}\right)} \right] \quad [5]$$

for water exhibits a break at 273 K i.e. its liquidus temperature (Figure 7a). These authors showed that values of liquidus temperatures could be derived for slags from viscosity data and these values were in line with recommended values (Figure 7b).

The concept was extended to a number of slags, including slags from mould fluxes, in order to determine the liquidus temperatures, as results from DTA measurements tend to be unreliable due to supercooling effects. In the case of the system $\text{CaO-Al}_2\text{O}_3\text{-FeO}$, the formation of a hitherto unknown ternary compound could be detected by this method²⁴. This is illustrated in Figure 8.

Experimental methods for viscosity measurements

A wide range of techniques has, over the years, been developed to measure the viscosity of various liquids at high temperatures. Due to the high temperatures involved in the determination, the following methods are usually adopted, viz. the capillary method, the falling body method, the oscillating methods, as well as the rotating cylinder method. The methods used for measuring viscosities of slags, glasses and fluxes are summarized in Table I.

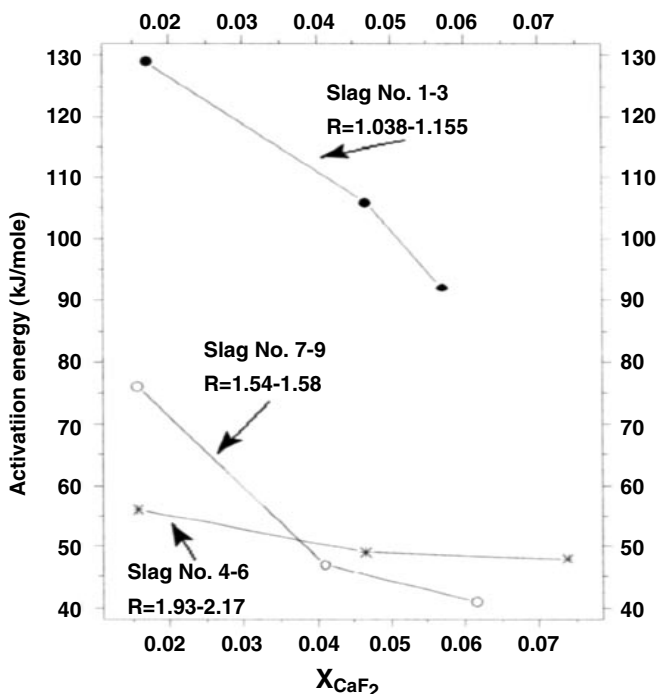
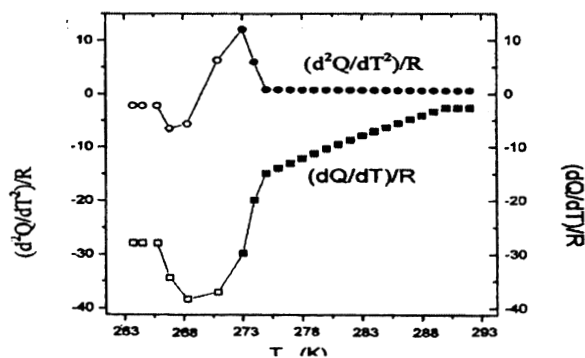


Figure 6. The effect of CaF_2 on the activation energies for viscous flow of fayalite slags with different $R (= X_{\text{FeO}}/X_{\text{SiO}_2})$ values⁶



The following three categories of experimental errors may deflect on the accuracy and thereby the reliability of the viscometric evaluations¹¹: (i) instrumental factors, (ii) material factors, and (iii) hydrodynamic factors. Instrumental factors relate to inadequate temperature control and geometric misalignment within the viscometer. Examples of material factors are inhomogeneities in the liquid due to improper mixing, molecular degradation, solvent evaporation, phase separation and particle agglomeration. Hydrodynamic factors involve flow instabilities, secondary flows, end effects and transient effects due to fluid elasticity. Any one, or a combination of, these factors can lead to significant errors and corresponding misinterpretation of the executed data. The most direct way to confirm the validity of measured viscosity data is to repeat the experiment on two devices with an overlapping shear-rate range, but with different operating modes.

The magnitude of several of these sources of uncertainty can be reduced by calibration with standard oils and high temperature reference materials. The present authors always calibrated the viscosity measurement system using the EU-reference slag, which consisted of $\text{Li}_2\text{O-Al}_2\text{O}_3\text{-SiO}_2$. With respect to the choice of crucibles and spindle materials, platinum 30% rhodium, molybdenum, ARMCO iron, as well as nickel were tried by the present authors and found that the measurement results were in agreement in all the cases. Some authors have used graphite components. The results obtained were often found to defer, due probably to either non-wetting conditions or occurrence of chemical reactions. Variations in reported viscosity values for laboratories using good practice are $<10\%$. Needless to point out, it is always important to confirm that the melt conforms to Newtonian behaviour.

Viscosity models

Several models have been reported for calculating the viscosity of melts from their chemical composition. The models of Riboud *et al.*²⁶ and Urbain²⁷ are some of the earliest models in viscosity estimations. Both these models utilize the advantages of the Wayman equation (Equation [3]). Riboud *et al.*²⁶ classified the slag components into five different categories, depending on their chemical nature, and attributed parameters to these categories. A different kind of classification of the slag constituents, viz. ‘glass formers’, ‘modifiers’ and ‘amphoterics’, was proposed by Urbain along with coworkers. This was later modified to calculate separate parameter values for different individual modifiers²⁸.

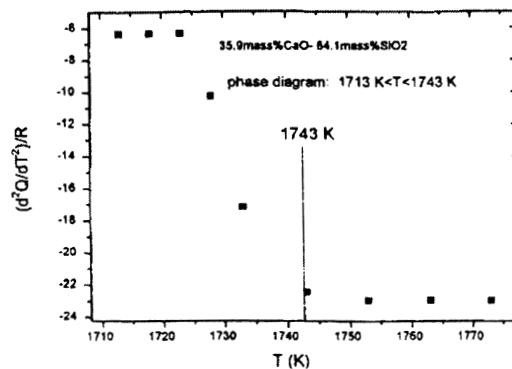


Figure 7. The second derivative of the activation energy as a function of temperature for (a) water and (b) slag ($\text{CaO } 35.9\% + \text{SiO}_2 \text{ } 64.1\%$)

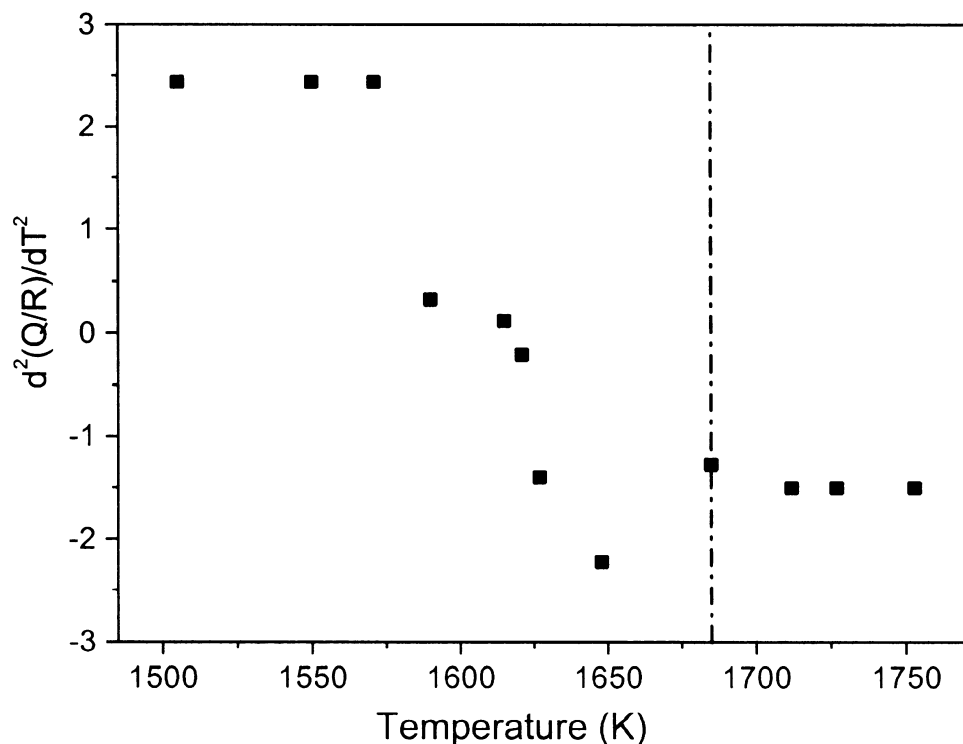


Figure 8: The second derivative of the activation energy divided by a constant (Q/R) as a function of temperature in the case of a slag containing 36 wt% Al_2O_3 , 31 wt% CaO and 33 wt% FeO

Table I
Methods used for measuring viscosities of slags, glasses and fluxes²⁵

Viscometer	Measurement	Range, Pa-s	Comment
Rotating crucible	Torque measured on static bob	10^1 – 10^2	Needs very accurate vertical alignment
Rotating bob	Torque measured on bob—several companies make viscometers	10^0 – 10^2	Alignment problems overcome using flexible joint
Falling body	Time for bob to fall (or drag) through known distance	$10^{0.5}$ – 10^5	Needs a long, uniform hot zone
Oscillating plate	Amplitude of plate in sample and air	$10^{-1.5}$ – 10^1	Need melt density value
Oscillating viscometer	Measures log decrement of amplitude of twisting	10^{-4} – 10^{-1}	1. Need melt density value 2. Roscoe Equation recommended
Shiraishi	Rotating plate-torque Parallel plate-sample height-time Indentation rate of penetration	10^2 – 10^{11}	
SLS	Damping of scattered waves on surface ('ripples')	10^{-5} – 0.5	Also measures surface tension

An excellent classification of the various viscosity models available and their salient features has been presented by Kondratiev *et al.*²⁹. It is seen in this classification that most of the modellers have preferred a Weyman-type of expression for the temperature dependence of viscosities. The reader is directed to this extensive review for further information. In the present paper, only a few of them are taken up for presentation.

In the modified Urbain model by 'Pyrosearch', Australia²⁹, the Urbain formalism has been revised and expanded so that separate model parameters can be included for the various chemical components. The major advantage of this modified Urbain model is that it enables the differences in chemistry of individual components to be taken into account while retaining the strength of the Urbain assumptions, i.e. the silicate slag viscosity increases with the third power of the glass former concentration and exhibits parabolic behaviour with varying proportions of amphoteric and network modifiers.

A quasi-structural approach towards the modelling of slag viscosities as functions of composition was utilized by a number of research groups. Among these, one of the significant models is that developed by Iida and coworkers³⁰. This model is based on an Arrhenius-type of equation, wherein a 'modified basicity index' accounts for the network structure of the slag. The amphoteric nature of oxides like alumina has been taken into consideration in the modelling. Zhang and Jahanshahi³¹ developed a model (CSIRO Model) for the estimation of viscosities of multicomponent slags. The temperature dependence of viscosities was described by the Weymann Equation [3]. The authors used a cell model for the description of the compositional dependency of the activation energy for viscous flow. Reddy and coworkers³¹ used a Weyman-type equation to describe the viscosities of slags. The compositional dependence was estimated by hole theory and atomic pair model.

Recently, Tanaka and coworkers³³ have developed a model for the estimation of viscosities of silicate melts. The model is based on an Arrhenius-type equation, wherein the activation energy was assumed to be inversely proportional to the total net movement of holes in unit time and volume. The net movement of the holes was based on the random walk theory.

A model for the estimation of viscosities of multicomponent slags was developed by the present authors at the Royal Institute of Technology³⁴. This model adopts the Arrhenius/Eyring equation for the description of viscosities. The activation energy for viscous flow was modelled in analogy with the modelling of Gibbs energy in thermodynamics. The model is now commercially available as a software, 'THERMOSLAG', and is being used by steel industries in a number of countries.

A summary of these models is given in Table II

Accurate viscosity and compositional data are needed to check the true capability of these models. A set of compositions for binary, ternary, quaternary, and multicomponent slags systems was distributed to the authors of various models²⁷⁻³⁵. The corresponding experimental results were obtained in the present laboratory by the rotating cylinder method using either Mo or Fe components. Calibrations of the systems were done periodically and the measurements were carried out under similar conditions. The experimental results are compared with the results of the calculations in Figure 9. It is to be noted that the model computations were carried out by the modellers themselves. The present authors have merely compiled the results.

It is seen in the above figures that, while the various models are able to approximately predict the order of magnitude of viscosities for the various systems, the actual values at a given temperature, as well as the temperature coefficients, differ significantly. In most cases, Iida's model is able to predict the viscosities close to the experimentation. The KTH model predictions also seem to predict the viscosities of the binary, ternary and quaternary slags reasonably well. The other models, except that of Tanaka, do not seem to deviate drastically from the experimental values. Professor Tanaka mentions in a private communication that his model needs further development and the results are to be considered as the first

stage of development. The present authors admit that there is a certain amount of bias in the comparison. The experimental values chosen for comparison were the values generated at the Division of Metallurgy, Royal Institute of Technology, Stockholm. The KTH model was 'trimmed' mathematically to these values and, hence, a reasonable agreement is naturally expected. In this respect, Iida's model could be considered to be quite reliable. Further, Iida's model can accommodate fluoride slags as well as coal ash slags.

The KTH model has recently been widened to include slags containing calcium fluoride. In these cases, fluoride was considered primarily associated with Ca²⁺. The experimental values are compared with the model predictions in Figure 10.

In the case of the available models for viscosity estimations of slags, it is to be pointed out that there are no a-priori models available that can cover the entire slag area. Most of the existing models are based on different mathematical expressions, based on semi-empirical approaches. Any comparison of the different models with respect to their performance are to be taken with great care since it is not certain whether, in the case of unknown slag compositions, the predictions can be reliable. In this respect, the authors would like to point out that greater effort is needed from the metallurgical community to generate reliable viscosity data so that the models can be tested. In the absence of stringent experimentation, comparisons of various model predictions towards the viscosities of complex slag at unknown temperatures is considered risky.

The viscosity values calculated by the Reddy model are not available for the slag compositions presented in the above figure. Some of the viscosity values reported by Reddy and coworkers are compared with the viscosities evaluated using the KTH model in Table III.

Several models have also been reported to estimate the viscosity in the super-cooled region of highly-polymerized slags. These models are based on:

- numerical analysis of viscosity-temperature-composition data.
- bond strengths of oxide glasses to enthalpy of formation of oxide ($\log \eta(\text{dPa}\cdot\text{s}) \approx 6$)
- viscosity-temperature relation to optical basicity (structure) with uncertainties in $\log_{10} \eta \leq \pm 0.5$.

Table II
Details of the methods used to estimate the viscosities of slags, glasses etc.²⁵

Reference	Method	Comment/applicability
Riboud ¹²	A_w and B_w as function of 'SiO ₂ ' 'CaO' 'Al ₂ O ₃ ' CaF ₂ and 'Na ₂ O'	Has been applied to wide range of slags Mould fluxes
Koyama ¹³	A_A and B_A as function of SiO ₂ , Al ₂ O ₃ , CaO, MgO, Na ₂ O, Li ₂ O, CaF ₂	Mould fluxes
Kim ¹⁴	A_A and B_A as function of SiO ₂ , Al ₂ O ₃ , CaO, MgO, Na ₂ O, Li ₂ O, B ₂ O ₃ , CaF ₂	Mould fluxes
Gupta ¹⁵	Constituents classified as network (1) formers (2) destroyers, and (3) fluorides η_T using T dependent constants	Mould fluxes
Mills ¹⁶	A_A and B_A as functions of Λ when corrected for charge balancing Al ₂ O ₃	Wide range of slags Mould fluxes
Urbain ¹⁷ Pyrohear ¹⁸	A_w and B_w as functions 'CaO' 'SiO ₂ ' and 'Al ₂ O ₃ ' - B_w values for MgO, MnO	Based on MO-Al ₂ O ₃ -SiO ₂ viscosities
Iida ¹⁹	Parameter, $\phi = \log(\eta/\eta_0)$ where η_0 derived from V^m, T^m and M and Basicity Index	Universal—performed well Mould slags Blast furnace slags, Coal slags
CSIRO ²⁰	A_w and E_w calculated as functions of N_0^0 and N_{O_2} - using MD calculations	For slags—SiO ₂ , CaO, MgO, Al ₂ O ₃ , FeO, Fe ₂ O ₃ , Coal slags
Tanaka ²² KTH ²³	Modified CSIRO model Thermodynamic model: B_A function of $\Delta G^*\eta = \sum(\Delta G^*\eta(\text{oxides}) + \Delta G^*_{\eta_{\text{mix}}})$ and $\Delta G^*_{\eta_{\text{mix}}}$ for interactions of cations only	For slags—SiO ₂ , CaO, MgO, Al ₂ O ₃ , CaF ₂ FeO, Fe ₂ O ₃ Synthetic slags

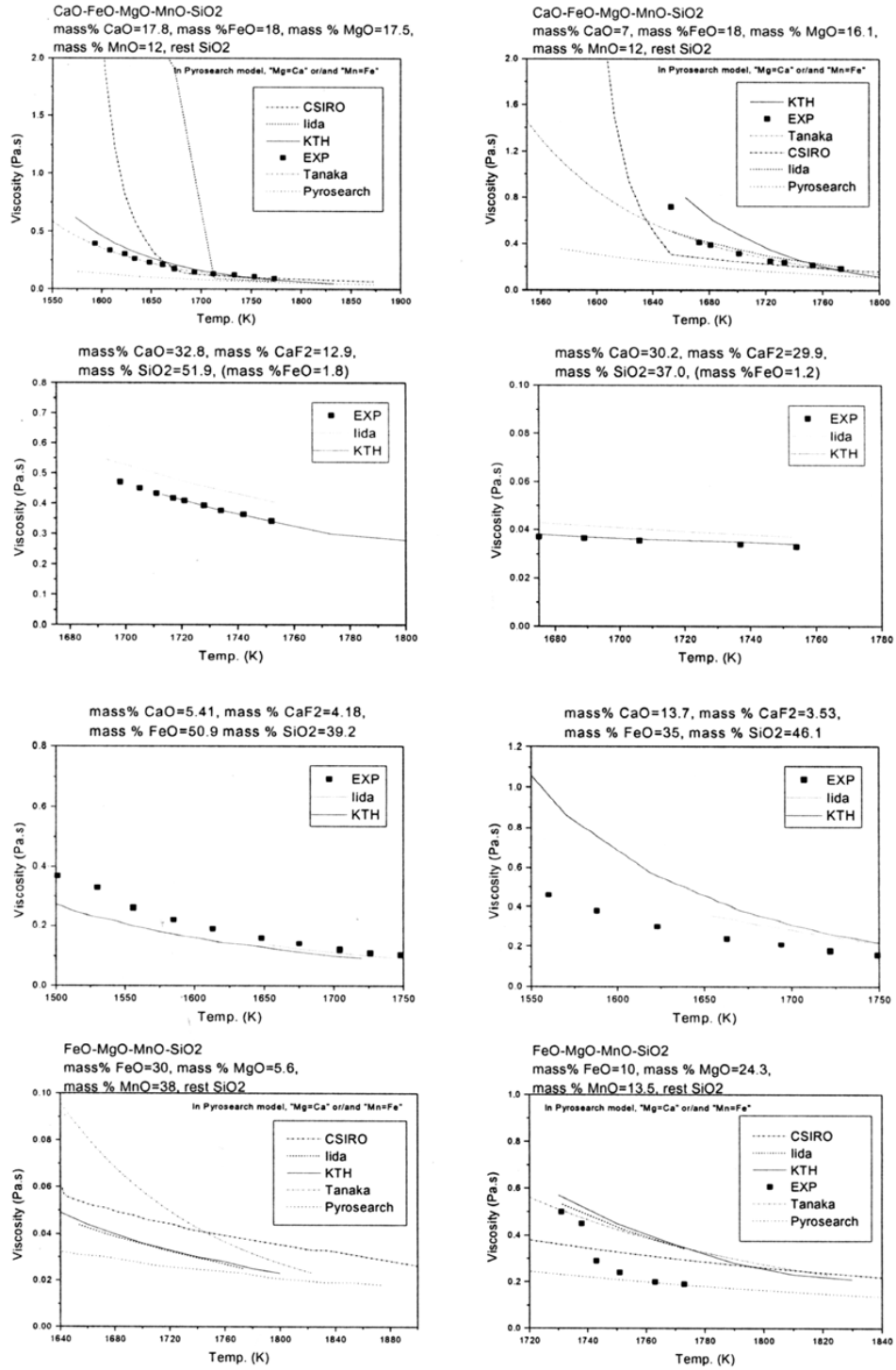


Figure 9. Comparison of the performance of various viscosity models^{26–34} with the experimental results

Surface viscosity

The following two kinds of surface viscosity are usually defined.

- Surface shear viscosity, ζ_s (MT⁻¹(dimensions)) given by the Equation [6].

$$\frac{\partial F}{\partial y} = \xi_s \frac{\partial v_x}{\partial y} \quad [6]$$

We generalize the above definition to the case of a fluid surface phase flowing in its own plane in the x direction with a uniform velocity v_x (y) direction by a pressure head F dyne/cm.

- Surface dilational viscosity (the area viscosity), ζ_s'' (MT⁻¹ (dimensions)), given by Equation [7]³⁴.

$$\Delta\gamma = \zeta_s'' \frac{1}{S} \frac{\partial S}{\partial t} \quad [7]$$

When the surface area S varies in such a way that, $\frac{1}{S} \frac{\partial S}{\partial t} = \text{const}$, ζ_s'' is obtained by measuring the corresponding change in the surface tension, $\Delta\gamma$ from Equation [7].

Equation [7] is analogous to Marangoni viscosity, ζ_M given with the following Equation [8].

$$\Delta\gamma = \zeta_M \frac{1}{S} \frac{\partial S}{\partial t} \quad [8]$$

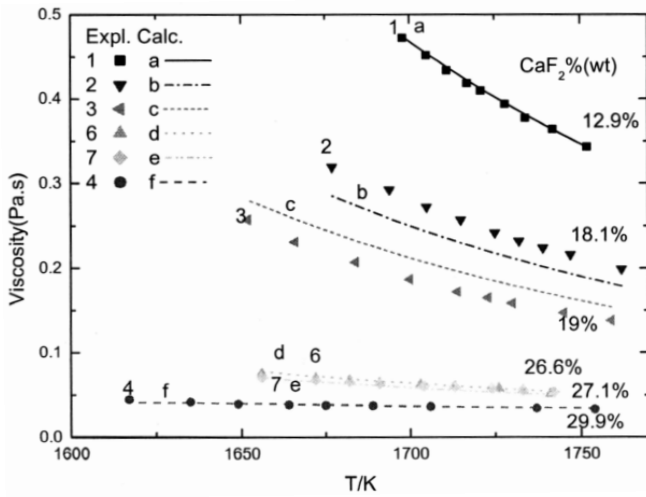


Figure 10. A comparison of the experimental viscosities with those predicted by the modified KTH-model in the case of the system CaO-SiO₂-CaF₂

Table III
Comparison between the viscosity estimations obtained from the models of Reddy *et al.*³² and KTH³⁴

System	Temp K	Mass%			Viscosity (Pa.s) Reddy	Viscosity (Pa.s) KTH
		CaO	MgO	SiO ₂		
CaO-MgO-SiO ₂	1773	CaO	MgO	SiO ₂		
		33.3	7.5	59.2	0.636	0.835
		30.8	13.3	55.8	0.339	0.557
FeO-MnO-SiO	1673	FeO	MnO	SiO ₂		
		60	20	20	0.032	0.0306
		50	30	20	0.032	0.0302
		50	10	40	0.201	0.149
		20	40	40	0.216	0.173
CaO-FeO-SiO ₂	1673	CaO	FeO	SiO ₂		
		8.7	46.3	45	0.317	0.223
		30	26.3	43.7	0.489	0.187
		26.3	30	43.7	0.512	0.177
		20	50	30	0.101	0.046
		31.2	38.8	30	0.091	0.066
		22.5	47.5	30	0.099	0.049

Therefore, ζ_s and ζ_M include the rate of attainment of equilibrium between the bulk phase and adsorbed surface (which contains Gibbs elasticity)^{35,36} as well as its own properties of adsorbed surface layer. In other words, the ζ_s and ζ_M may be called 'Gibbs-Marangoni' viscosity.

The above-mentioned two kinds of surface viscosity are reasonable and useful in order to understand and to analyse the interfacial phenomena.

Surface dilational viscosity is closely related to the following interfacial phenomena: foaming, coalescence of bubbles, droplets and solid particles in liquid, and also dispersion of bubbles, droplets as well as solid particles into liquid. The involvement of mould powder or slag by the molten steel should also be influenced by ζ_M . All of the above-mentioned phenomena include the elemental processes of (i) surface (interface) expansion or shrink, (ii) drainage, and (iii) break of the melt film.

It should, however, be very hard to apply the measuring methods that were previously developed for the room temperature liquids system³⁵ to the high temperature melt system.

The optimum procedure would first be to clarify the mechanism of the interfacial phenomena and the extent of participation of surface dilational viscosity in the phenomena. Secondly, it is necessary to develop a suitable or useful measuring method for surface dilational viscosity.

Two-phase viscosities

When two immiscible liquids, one with a low viscosity and another with a high viscosity liquid, are brought together, it results, rather surprisingly, in an increase in overall viscosity (η_{eff}). Relations have been developed by Einstein and by Taylor, which are given in Equations [9] and [10] respectively.

$$\eta_{eff} = \eta(1 + 2.5c) \quad [9]$$

$$\eta_{eff} = \eta(1 + c\{1 + 2.5\lambda/1 + \lambda\}) \quad [10]$$

where η = viscosity of fluid, η_p and c are viscosity and volume fraction of disperse phase and $\gamma = \eta_p/\eta$. Recent results for the addition of water (disperse phase) to silicone oils show (Figure 11) that the experimental data fall between the two equations for the range $0 < c < 0.237$.

Dynamic viscosity measurements

Since viscous flow is related to the structure of the liquid, following the viscosity of a liquid would provide useful information of the progress of a reaction, wherein a structural change is involved. For example, one could monitor the fluoride losses or alumina dissolution by monitoring the viscosity increase of the mould flux slag. The viscosity variation of the slag of copper metallurgy would reveal the oxidation of slag, as the increase of the Fe³⁺ leads to an increase in the slag viscosity.

Figure 12 presents the viscosities of a slag (40% CaO, 5% FeO-50% SiO₂-5% CaF₂) at 1714 K, 1740 K and 1757 K as functions of time while alumina gets dissolved into it.³⁹ The process was found to be controlled by dissolution of the protecting layer formed on the surface of the alumina disc accompanied by the diffusion of Al₂O₃ into the slag after the initial stages.

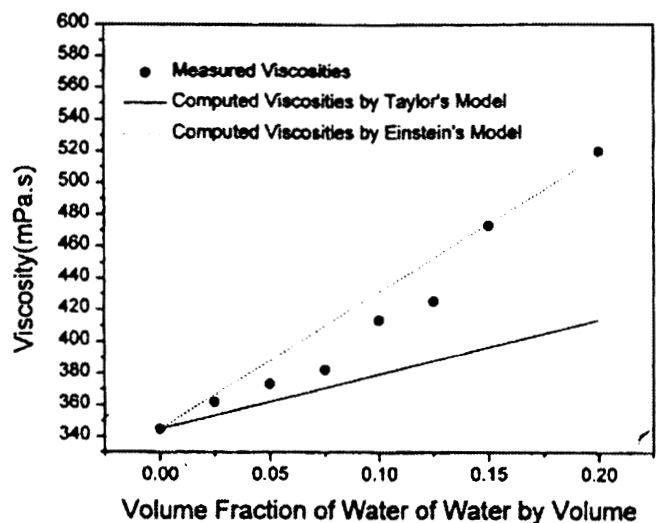


Figure 11. Overall viscosities of (silicone oil + water mixtures) as a function of volume fraction of H₂O comparing calculated with measured values³⁷

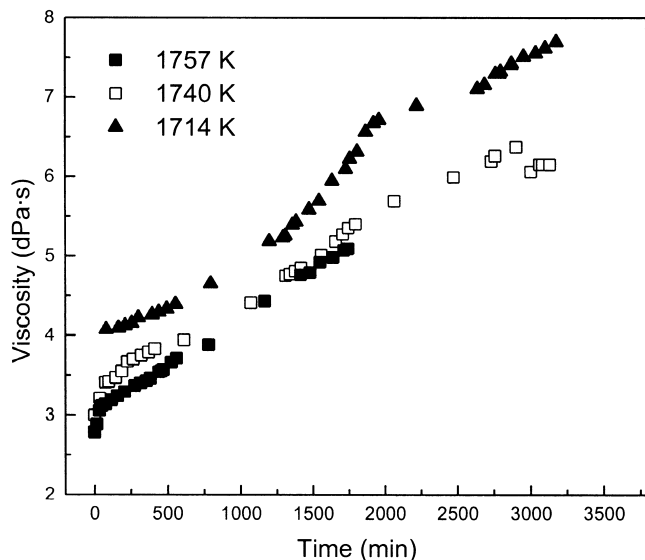


Figure 12. The change of slag viscosities as a function of time due to alumina dissolution.³⁸

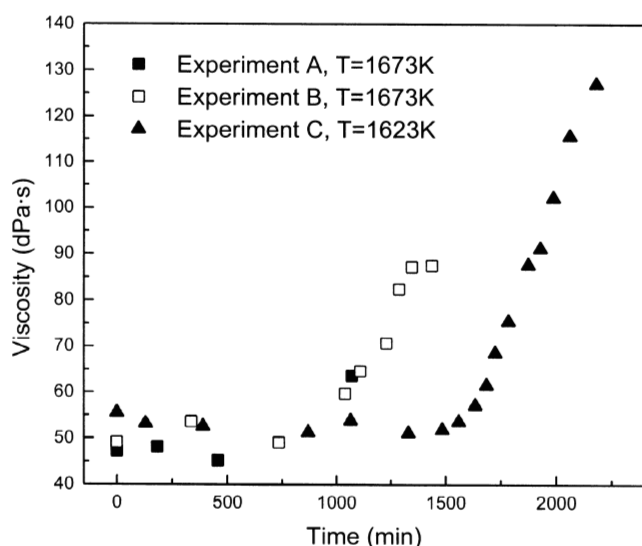


Figure 13. Viscosity changes during the oxidation of a fayalite slag.³⁹

Figure 13 shows the measured viscosity varying with time at 1673 and 1623 K, when a binary $\text{Fe}_n\text{O-SiO}_2$ slag is exposed to a CO-CO_2 mixture.³⁹ The ratio of P_{CO_2} to P_{CO} was 9.81, which would lead to oxygen partial pressures of $2.5 \cdot 10^{-7}$ atmosphere at 1673K and $7.2 \cdot 10^{-8}$ atmosphere at 1623K. It can be seen that reasonable reproducibility of measurements has been reached. The viscosity of the slag almost remains the same during the initial part of oxidation with a slight decrease at 1623 K. At longer oxidation time, there is a sharp raise in viscosity. This rise in viscosity occurs earlier at 1673 compared to that at 1623 K.

Application of viscosity data in process simulation

Using reliable physical property data is the foremost condition for any meaningful process simulation. This aspect has been elaborated by Jönsson *et al.*⁴⁰ The application of the reliable viscosity data in the model of sulphur refining in a gas-stirred ladle has shown promising results.¹ Figure 14 shows the change of sulphur concentration in steel during refining, when 80 l/min argon gas is injected into 100 ton of steel. Argon is injected through a centrally located porous plug in the bottom of the ladle. Since the ladle is axially symmetric, only half of the ladle is shown in the two-dimensional plane in the figure.

The predicted sulphur content in the steel for this case is 0.007 wt% to 0.008wt% after 15 minutes of gasstirring. Actual plant data for a 15 minutes gas-stirring period with the same gas flow gives a sulphur content of 0.005 wt% to 0.010 wt%. However, it is very difficult in a plant situation to know if the gas flow is constant during injection. Very often gas leaks out through cracks in the refractory, etc. However, the rough comparison shows that by using accurate slag data in a CFD model of a gas-stirred ladle, it is possible to predict desulphurization with acceptable accuracy.

Summary

The present keynote paper presents an overview of slag viscosities, their importance in process simulations, and the linking of viscosities with the structure of slags. The dependence of slag viscosities on composition and temperature are discussed. Experimental methods of measuring slag viscosities are presented along with their limitations. The various models for the estimation of slag viscosities are presented and their relative performances are

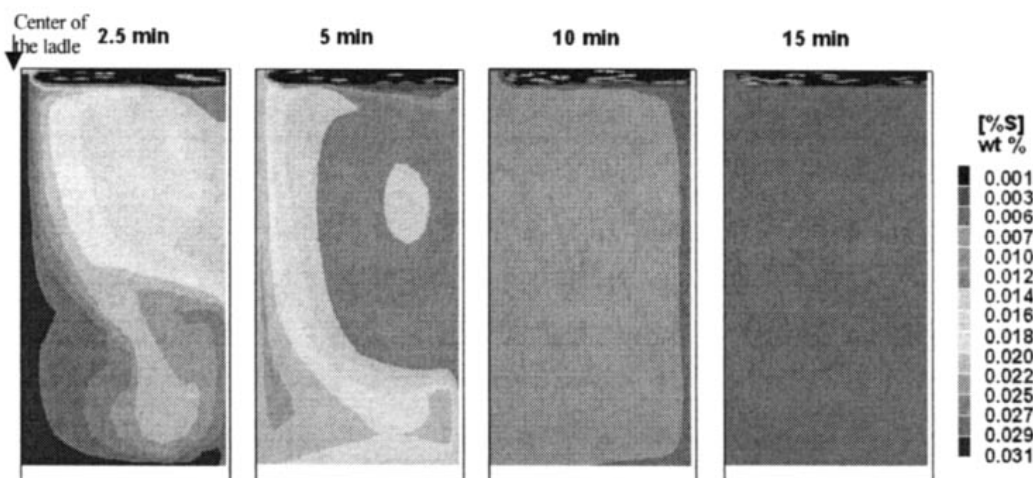


Figure 14. Change of sulphur content in steel as a function of refining time.¹

analysed in comparison with experimental data in the case of binary, ternary, and multicomponent slags. The concept of surface viscosity is taken up as two-phase viscosities.

References

1. JONSSON L., SICHEN, D., and JÖNSSON G.P. *ISIJ International*, vol. 38, 1998, pp. 260–267.
2. JI, F-Z., SICHEN, D., and SEETHARAMAN, S. *International J of Thermophysics*, vol. 20, 1999, p. 541.
3. JI, F-Z., SICHEN, D., and SEETHARAMAN, S. *Metall. Materials Trans. B*, vol. 28B, 1997, pp. 827–34.
4. JI, F-Z., SICHEN, D., and SEETHARAMAN, S. *Ironmaking and Steelmaking*, vol. 25, 1998, pp. 309–316.
5. SHAHBAZIAN, F., SICHEN, D., MILLS, K.C., and SEETHARAMAN, S. *Ironmaking and Steelmaking*, vol. 26, 1999, pp. 193–199.
6. SHAHBAZIAN, F., SICHEN, D., and SEETHARAMAN, S. *ISIJ International*, vol. 39, 1999, pp. 687–696.
7. SHAHBAZIAN, F. *Scandinavian Journal of Metallurgy*, vol. 30, 2001, pp. 302–308.
8. SHAHBAZIAN, F., SICHEN, D., and SEETHARAMAN, S. *ISIJ International*, vol. 42, 2002, pp. 155–162.
9. RICHARDSON, F.D. *Physical Properties of Melts in Metallurgy*, Academic Press, London, 1974.
10. BORN, M. and GREEN, H.S. *A General Kinetic Theory of Liquid*, Cambridge University Press, London, 1949.
11. McCAULEY, W.L. and APELIAN, D. *Proc. of 2nd Int. Conf. on Metallurgical Slags and Fluxes*. Fine, H.A. and Gaskell, D.R. (eds.) Metall. Soc. AIME Warrendale, PA, USA, 1984 p. 925.
12. IIDA, T., UEDA, M., and MORITA, Z. *Tetsu-to-Hagané* vol. 62, 1976, pp. 1169–78.
13. MORITA, Z., IIDA, T., and UEDA, M. *Liquid Metals, Inst. Phys. Conf. Ser.* no. 30, Bristol. 1976, pp. 600–606.
14. SEETHARAMAN, S. and SICHEN, D. *Metall. Mater. Trans. B*, vol. 25 B, 1994, pp. 589–595.
15. SEETHARAMAN, S., SICHEN, D., and JI, F-Z. *Metall. and materials. Trans. B*, vol. 31B, 1999. pp. 105–09.
16. MEHTA, S. and RICHARDSON, F.D. *J. Iron Steel Inst.*, vol. 203, pp. 524–28.
17. SRIDHAR, S., SICHEN, D., SEETHARAMAN, S. and MILLS, K.C. *Steel research*, vol. 72, 2001. pp. 3–10.
18. DARKEN, L.S. *TMS-AIME*, vol. 239, 1967, pp. 80–89.
19. AUNE, R.E., HAYASHI, M., and SRIDHAR, S. Accepted for publication in *High temp. Mater. Proc.*, 2003.
20. FUJINO, S. and MORINAGA, K. *J Non-Cryst. Solids*, 2003, in press.
21. URBAIN, G. and BOIRET, M. *Ironmaking and Steelmaking*, vol. 17, 1990, pp. 255–260.
22. McCAULEY, W. L. and APELIAN D. *Proc. of 2nd Int. Conf. on metallurgical slags and fluxes*. Fine, H. A. and Gaskell, D.R. (eds.), held at Lake Tahoe, Nev., Publ. Met. Soc. AIME Warrendale, Pa. pp. 925-947.
23. SEETHARAMAN, S., SRIDHAR, S., SICHEN, D., and MILLS, K.C. *Metall. Trans. B*, vol. 31B, 2000, pp. 111–119.
24. VIDACAK, B., SICHEN, D., and SEETHARAMAN, S. *ISIJ International*, vol. 42, 2002, pp. 561–63.
25. MILLS, K.C. and SEETHARAMAN, S. *Huttenpraxis Metallweiterver. Iida Commomerative Special Issue*, Osaka Univ., Japan, May 2003. Riboud, P.V., Roux, Y., Lucas, L.D., and Gaye, H. Fachber (eds). vol. 19, 1981, p. 859.
26. RIBOUD, P.V., ROUX, Y., LUCAS, L.D., and GAYE, H. *Fachber. Huttenpraxis Metallweiterver.* vol. 19, 1981, p. 859.
27. URBAIN, G. *Rev. Int. Haut. Temp. Refract.*, vol. 11, 1974, pp. 133–145; Urbain, G. *J. Mater. Educ.*, vol. 7, 1985, pp. 1007–1078; Urbain, G. *Steel Research* vol. 58, 1987; Urbain, G. and Boiret, M. *Ironmaking & Steelmaking*, vol. 17, 1990, pp. 255–260.
28. KONDRATIEV, A., JAK, E., and HAYES, P.C. *J. Met.*, 2002, pp. 41–45; Kondratie, A., and Jak, E. *Metall. Mater. Trans B*, vol. 32B, 2001, pp. 1015–1025; Kondratiev, A., and Jak, E. *Fuel*, vol. 80, 2001, pp. 1989–2000.
29. IIDA, T. *Proc. Mills Symposium*, Aune, R.E. and Sridhar, S. (eds.) publ. NPL, Teddington, UK, 101/111, Iida, T., Sakai, H., Kita, Y.. and Shigeno, K. *ISIJ Intern.* vol. 40, 2000, pp. S110–S114., Iida, T. and Kita, Y. *The 19th Committee, JSPS, Rept.* no. 11949, Jan. 2002.
30. ZHANG, L. and JAHANSHAH, S. *Met Trans B*, vol. 29B, 1998, pp. 177–186.
31. HU, H. and REDDY, R.G. *High Temp. Sci.*, vol. 28, 1990, pp. 195–202; Reddy, R.G. and Hebbbar, K. 1991, *TMS EPD Congress*, pp. 523–540; Zhang, Z. and Reddy, R. *EPD Congress TMS*, pp. 957–970, Reddy, R.G. and Hebbbar, K. *Minerals & Metall. Proc.*, vol. 18, 2001, pp. 195–199; Hebbbar K.M.S thesis, Univ. of Nevada, Reno, USA, 1991.
32. LEE, J., NAKAMOTO, M., and TANAKA, T. Communicated to *ISIJ International*, 2003.
33. SEETHARAMAN, S., SICHEN, D., and ZHANG, J.Y. *J Metals*, vol. 51, no. 8, 1999, pp. 38–40.
34. VADER, F., VAN VOORST, ERKENS, T.F., and TEMPEL, M. Van Den. *Trans. Faraday Soc.*, vol. 60, 1964, p. 1170.
35. KITCHENER J.A. *Nature*, vol. 194, 1962, p. 676.
36. KITCHENER J.A. *Nature*, vol. 195, 1962, p. 1094.
37. LIU, W., SICHEN, D., and SEETHARAMAN, S. *Met Trans*. vol. 32B, 2000, p. 110.
38. SHAHBAZIAN, F., SICHEN, D., and SEETHARAMAN, S. *ISIJ International*, vol. 42, 2002, pp. 155–62.
39. VISWANATHAN, N.N., JI, F-Z., SICHEN, D., and SEETHARAMAN, S. *ISIJ International*, vol. 41, 2001, pp. 722–27.
40. JÖNSSON, P.G., JONSSON, L., and SICHEN, D. *ISIJ International*, Japan, vol. 37, 1997, pp. 484–91.

